Published in final edited form as:
J Biomed Mater Res A. 2010 December 15; 95(4): 1055–1066. doi:10.1002/jbm.a.32904.

Biomimetic Matrices for Myocardial Stabilization and Stem Cell Transplantation

Samuel T Wall[1], **Che-Chung Yeh**[2], **Richard YK Tu**[2], **Michael J. Mann**[2,3], and **Kevin E Healy**[1,4,*]

[1]University of California at Berkeley, Department of Bioengineering

[2]Department of Veterans Affairs Medical Center, San Francisco, California

[3]University of California at San Francisco, Department of Surgery

[4]University of California at Berkeley, Department of Material Science and Engineering

Abstract

Although natural biological matrices have demonstrated modest improvement in the survival of cells transplanted into the infarcted myocardium, these materials have not been amenable to systematic optimization and therefore have limited potential to treat post infarct cardiac injuries. Here we have developed tunable bioactive semi-interpenetrating polymer network (sIPN) hydrogels with matrix metalloproteinase (MMP) labile crosslinkers to be used as an assistive microenvironment for transplantation of bone marrow derived mesenchymal stem cells (BMSCs) into the infarcted myocardium. Injectable sIPN hydrogels were designed with a range of mechanical and biological properties that yielded material-dependent BMSC proliferation *in vitro*. Five groups were evaluated to treat myocardial infarction (MI) in adult mice: saline injection; green fluorescent protein (GFP)(+)-BMSCs delivered in saline; a sIPN matrix; a sIPN + GFP(+)-BMSCs; and Matrigel™ + GFP(+)-BMSCs. Injection of cells alone created a transient improvement in LV function that declined over time, and the synthetic hydrogel without cells resulted in the highest LV function at 6 weeks. Donor GFP-positive cells were detected after matrix-enhanced transplantation, but not without matrix support. Biomimetic sIPN hydrogel matrices succeeded both in mechanically supporting the injured myocardium and modestly enhancing donor cell survival. These matrices provide a foundation for systematic development of "pro-survival" microenvironments, and improvement in the long-term results of cardiac stem cell transplantation therapies.

Introduction

Acute damage wrought by myocardial infarctions (MIs) continues to combine with post-MI remodeling to result in heart failure for many patients. To date, no treatments have succeeded in preventing or reversing the progression of heart failure; therefore, new techniques, such as biomaterial based tissue engineering, are urgently needed. This approach may involve innovatively designed biomaterials, transplantation of stem cell populations, and novel surgical methods in an attempt to stabilize an injured ventricle and hopefully replace lost cardiomyocytes in order to regenerate a working myocardium.

*Correspondence to: Professor Kevin E. Healy, University of California, Berkeley, 370 Hearst Memorial Mining Building, #1760, Berkeley, CA 94720, kehealy@berkeley.edu, Telephone: 510 643-3559, Fax: (510) 643-5792.

Disclosures
Authors have disclosed no conflict of interest.

Stem cell transplantation to the damaged left ventricle (LV) has received widespread attention in the last decade, and numerous preclinical[1-5] and early clinical[6-8] studies have been reported. Despite the encouraging preliminary results obtained with numerous types of transplanted cells, including bone marrow derived mesenchymal stem cells (BMSCs),[3,9,10] endothelial progenitor cells,[2] resident cardiac stem cells,[11,12] and embryonic stem cells,[13] definitive demonstration of functional regeneration of an organized myocardium remains an unmet goal. As the survival of transplanted cells has come under scrutiny,[14,15] the addition of extracellular matrices (ECMs) to provide a suitable microenvironment for the implanted cells has been explored, and has included such biomaterials as fibrin based glue,[16] the biologically derived basement membrane material Matrigel™,[13,17] collagen foam,[18] alginate,[19] and peptide-based associative networks.[20,21]

In addition to any benefits associated directly with increased cell survival after transplantation, the injection of material even without cells may improve post-MI ventricular function. Recently, we have reported a theoretical mathematical model of matrix-assisted myocardial stabilization (MAMS),[22] demonstrating that injection of non-contractile material with a wide range of mechanical properties in the border zone (BZ) of the infarct can reduce elevated wall stresses. This work suggested that injection of biomaterials in the left ventricle might attenuate post-infarct myofiber stresses and ameliorate both ventricular remodeling and infarct extension. These simulated results fit well with recent experimental studies that used materials such as Matrigel™,[13] collagen, [23] fibrin,[16] alginate,[24,25] and synthetic polymers[26-28] to treat the injured heart, all of which have demonstrated modest improvements in heart function compared to saline controls in the absence of added cells.

In order to provide more rigorous control of ECM materials for tissue engineering applications, we have chosen to create a biomimetic polymer, a synthetic hydrogel modified with short amino acid sequences to reproduce specific biological functionality of the natural ECM such as cellular attachment points and injury driven remodeling capacity. The base polymer system we utilized for these modifications is referred to as a semi-interpenetrating polymer network (sIPN), and we exploited the unique properties of sIPNs to test the hypotheses that injected materials, with or without cells, can support the injured myocardium. Furthermore we also tested the hypothesis that by designing modified, biomimetic sIPN systems that support donor cell proliferation, the persistence of transplanted cells in the myocardium can be enhanced. The sIPNs used in this work contained a crosslinked copolymer network of N-isopropylacrylamide and acrylic acid, similar to hydrogels used in cardiac work previously, [26,28] but interpenetrated with linear chains of polyacrylic acid with chemically tethered peptides that engage with cell-surface integrin receptors (i.e., $\alpha_v\beta_3$),[29-32] encouraging cellular attachment and presenting a known angiogenic motif.[33] When polymerized in aqueous solution, this polymer forms a loosely crosslinked and highly hydrated hydrogel that has the ability to sustain the growth of a cell population[30-32] across a wide range of controllable mechanical properties. In the context of cardiac bioengineering, control of mechanical properties in the cellular milieu is of increasing importance as it has been shown to affect proliferation and differentiation of numerous cell types, including adult mesenchymal stem cells.[32,34-36] Within this hydrogel, cells can be entrained for direct injection into the injured myocardium, after which the material warms and stiffens in place due to a lower critical solution temperature (LCST) phase change.[37,38] Due to the added AAc polymer units, the change in volume is low following this LCST transition to prevent swelling or collapse of the network. Following implantation, this material is designed to take advantage of the myocardium specific microenvironment, degrading through cell-based proteolytic action on the matrix metalloproteinase (MMP)-labile peptide sequences which crosslink the polymer chains.

Methods and Materials

sIPN Hydrogel Synthesis

Thermoresponsive poly(N-isopropylacrylamide-co-acrylic acid) [p(NIPAAm-co-AAc)] hydrogels with MMP peptide degradable crosslinkers were produced through free radical addition polymerization similar to previously described methods (Figure 1, A).[30-32] All peptides used in this study were custom synthesized by American Peptide Co. (Sunnyvale, CA) and characterized using mass spectrometry and HPLC (purity > 95 %). Briefly, NIPAAm and AAc monomers (Polysciences Inc, Warrington, PA) in a 95:5 molar ratio, along with 0.3 mol% of a diacrylated MMP labile peptide sequence (Ac-GPLGLSLGK-NH_2, see below) were dissolved at 3 – 5 wt% in incomplete phosphate buffered saline (iPBS). Polyacrylic acid (pAAc) linear chains (450 kDa) grafted with a 15 amino acid bone sialoprotein derived -RGD- peptide sequence (Ac-CGGNGEP**RGD**TYRAY-NH_2, referred to as **bsp-RGD(15)**), synthesized as described previously,[30,32] were then added in the 0 – 0.8 mg/mL range (corresponding to a -RGD-peptide concentration of ~ 0 – 100 μM). The resulting solutions were degassed with dry N_2, mixed with the free radical initiator ammonium persulfate (AP) and the accelerator N,N,N′,N′-tetramethylethylenediamine (TEMED), and allowed to polymerize overnight under N_2. After polymerization, the hydrogels were washed of unreacted monomers by thorough sequential rinses in iPBS combined with cycling through the hydrogel's LCST.

MMP labile crosslinker

In order to establish control of the degradation rate of the gel, the peptide crosslinking sequence previously used in the MMP labile sIPN hydrogels (i.e., Ac-QPQGLAK-NH_2)[31] was varied and tested against a panel of MMPs known to be upregulated in the injured rodent heart (e.g., MMP-2, -9, and -13).[39] In addition to the original sequence initially studied two other sequences were chosen from published studies of MMP labile sequences[40] that would be suited for diacrylation: Ac-GPLGLSLGK-NH_2 and Ac-GPLGMHGK-NH_2. Proforms of MMP-13, MMP-9, and MMP-2 were obtained (R&D Systems) and activated using p-aminophenylmercuric acetate (APMA) according to the manufacturer's protocols. Peptide substrate sequences were then dissolved at varying concentrations in TCNB buffer and incubated with a constant amount of activated MMPs. At time points ranging between .5 – 4 hrs, samples of the reaction were removed and mixed with equal volumes of 0.1% heptafluorobutyric acid to quench the MMP reaction. The set of samples were then assayed via high performance liquid chromatography (HPLC) to determine the remaining concentration of uncleaved protein. Change in concentration was used to calculate reaction rate, and Michaelis-Menton kinetic parameters were then computed through direct non-linear regression analysis (MATLAB software, Mathworks, Inc, Natick, MA) on the reaction rate as a function of substrate concentration.

Mechanical Characterization

Mechanical properties of the hydrogels synthesized at varying polymer weight percentages were tested using parallel plate rheology. For each synthesized material, 3 mL of hydrogel was loaded onto a temperature controlled rheometer (MCR300, Anton Paar, Ashland, VA) with 50 mm sandblasted parallel plates, and the complex modulus of the materials determined using a 5% dynamically loaded strain at a gap height of 1.0 mm. Sample modulus was first measured across a range of frequencies (0.01 – 14 Hz) at 22°C, then the sample was slowly warmed to 37°C, and the frequency again swept to test the mechanical properties after the LCST. In addition to mechanical testing, sIPNs were tested by surgeons to examine their injectability. All the hydrogels produced were loaded into 1 mL syringes with a range of needle sizes to test how well small volumes of the materials could be delivered.

Cell Isolation and Characterization

We used an established cell culture system to maintain and expand well-characterized green fluorescent protein (GFP)-expressing C57Bl mouse BMSCs *in vitro*. Briefly, marrow was flushed from the tibia and femur of adult GFP transgenic mice (8-12 weeks of age) and subjected to density centrifugation to eliminate many of the mature leukocytes. BMSCs are known to preferentially attach to polystyrene surfaces, and differential plating was used to eliminate hematopoietic cell lineages. BMSCs were propagated in alpha minimum essential medium (αMEM), with Glutamax plus 10% fetal bovine serum until reaching a logarithmic phase of cell growth. These bone marrow-derived cell lines have been associated with a pattern of stem cell marker expression consistent with the reported literature, including CD-90, CD-71, and CD-117, but not hematopoietic markers CD-34 or CD-45.

Hydrogel Cell Culture

For three dimensional (3D) cell culture studies, hydrogels were synthesized in the characterized stiffness range of 3 – 5% total polymer content in the same monomer ratios as above. Synthesized pAAc-graft-bspRGD(15) was incorporated into the gels at 0 mg/mL, 0.4 mg/mL and 0.8 mg/mL, giving bulk concentrations of 0, ~50 μM and ~100 μM. Polymerizing hydrogel solutions were mixed as was done for the bulk synthesis, and then 200 μL aliquots of the reacting solutions were pipetted quickly onto methoxysilane treated glass coverslips in order to create a permanent bond between the surface and the forming polymer network. After overnight polymerization, hydrogel samples were rinsed 3× in iPBS and sterilized by 30 minute incubation in 70% EtOH.[41] They were rinsed again 3× in sterile iPBS followed by equilibration in culture media (αMEM w/o nucleosides, 10% FBS, 2mM L-glutamine, and antibiotics) at 37°C for 4 hours.

To seed the hydrogel samples, GFP+ BMSCs were suspended at a concentration of 10^6 cells/mL, and 200 μL total of this solution containing 2×10^5 cells was injected into the coverslip bound hydrogels in a series of 15 – 20 small volume injections using a 23 gauge needle. These cell-loaded hydrogels were then placed into 16 well tissue culture plates and 1.5 mL of warm media was added to each well. Samples were incubated at 37°C in 5% CO_2 for 14 days, with media changed every 2 – 3 days, and hydrogels removed at 1, 4, 7, and 14 days. Hydrogel samples were then visualized using a fluorescent microscope, homogenized using hand held small volume homogenizer, and assayed for cell number using the Cyquant GR assay (Molecular Probes, Eugene, OR) against generated cell number standards. Cell proliferation as a function of stiffness and RGD content at day 14 was mapped to a response surface by fitting the data to a quadratic curve using MATLAB software.

Mouse Infarct Model and Injections

An sIPN formulation of 4% 95:5 p(NIPAAm-co-AAc) with 0.3 mol% crosslinker content and 50 μM RGD was synthesized for direct injection with or without BMSCs. This formulation was specifically chosen from *in vitro* results in order to maximize cell growth in the matrix while maintaining cell/matrix interaction within the limitations of the animal model employed (see, Results). EGFP-expressing BMSCs were grown to near confluence, trypsinized, counted, and pelleted in a microfuge tube. Sufficient quantities of prepolymerized hydrogel were then pipetted into the tube and mixed with a spatula to achieve a cell density of 10^7 cells/mL. The cell / gel mixture was microscopically visualized to assure an even distribution of cells within the matrix, and was kept at 4°C until injection. As a comparative matrix control, the same procedure was used with cold, liquid growth factor-reduced, phenol red-free Matrigel™ (BD Biosciences, San Jose, CA) to make an injectable cell / gel mixture. A control suspension of cells in sterile saline was also prepared at the same cell concentration.

Male C57Bl/6 mice (6-8 weeks old) were anesthetized with pentobarbitol prior to intubation with a 24 gauge angiocatheter. Inhalation anesthesia was then instituted with 1.5% isoflurane using a rodent ventilator (Harvard) at 115 breaths/min. A left lateral thoracotomy incision was placed at the level of the fourth interspace and a 6-0 polypropylene suture was used to ligate the left anterior descending (LAD) artery at approximately 1/3 the distance from the base to the apex of the heart. Blanching of the distal left ventricular wall was observed to verify ligation. Immediately after generation of the infarct, inhalation anesthesia was reduced and 10 μL of the test material was injected into the anticipated infarct border zone region of the LV wall in a single injection using a 30 gauge needle. Animals were ventilated for approximately 15 minutes after chest closure, and were then recovered in a light-warmed incubator. Animals in the sham surgery group underwent thoracotomy without LAD ligation.

Transthoracic echocardiography was performed at 2, 4, and 6 weeks after MI on conscious, gently restrained mice using an Acuson Sequoia 512 machine and a 13-MHz probe. A two-dimensional short-axis view of the left ventricle was obtained at the level of the papillary muscles, and two-dimensional M-mode tracings were also recorded. LV fractional shortening (FS) was calculated as (Dd –Ds) / Dd and LV ejection fraction (EF) as (LVEDV-LVESV) / LVEDV, where Dd = LV diastolic dimension, Ds = LV systolic dimension, LVEDV = LV end-diastolic volume, and LVESV = LV end-systolic volume. LV volume was calculated as (short axis length)^2 × (long axis length) × 0.654.

Mice were sacrificed at 6 weeks post-MI. Thin frozen sections were obtained to preserve the GFP signal of the implanted cells, which, when present, could be detected easily via fluorescent microscopy of the ventricle wall. For each heart, sections were taken every 200 microns from the apex of the ventricle to the point of LAD ligation. Adjacent sections were stained using Gomori's trichrome, and image analysis software (ImageJ, NIH) was used to determine the thicknesses of both the infarcted and the remote, uninfarcted left ventricular wall, as well as the extent of infarction.

Statistics

All statistical differences between time points and between groups were determined by one way analysis of variance followed by Tukey HSD post-hoc tests. Data are reported as mean ± SEM, and a P-value of less than 0.05 was considered to denote statistical significance.

Results

MMP Labile Crosslinkers

Michaelis-Menten parameters (V_{max}, K_m) for the MMP labile crosslinking sequences are shown in Table 1, along with the selectivity and ratio of the selectivity to the most slowly degrading sequence. Between the three sequences, selectivity spanned two orders of magnitude against MMP-13 and one order of magnitude for MMP-9 and MMP-2, providing a specific means of controlling degradation rates in varying microenvironments.

sIPN hydrogel Characterization

Hydrogels were made with controllable mechanical properties, having a complex shear modulus spanning 95 – 155 Pa at biological temperature and relevant cyclical loading ranges (Figure 1, B, filled markers). At this temperature (37°C), there was also a significant qualitative difference between the formulations; the 3% sIPN behaving very soft and pliable while the 5% gel was much stiffer. The mechanical properties of all the formulations at room temperature differed substantially from those measured at 37°C, with very low moduli (Figure 1,B, open markers) and high loss angles (data not shown) that allowed them to be

passed through small gauge needles. However, there was a change in room temperature stiffness between the 4 wt% and 5 wt% polymer compositions, and while all formulations could easily pass through larger gauge needles, clinicians reproducibly detected a difference in pressure required during delivery through a 30 gauge needle for high weight percent sIPNs. Due to the limitations of the animal model, where fine control was needed to inject into the thin wall of the mouse, the surgeons preferred sIPNs less or equal to 4 wt% for the *in vivo* studies.

In Vitro Cell Culture

In vitro cell proliferation varied as a function of matrix stiffness and bsp-RGD(15) content (Figure 2, A). All sIPN formulations were able to sustain cell growth over 2 weeks as reflected by increased cell number; however, the integrin-binding peptide concentration and the material stiffness influenced the rate of cell growth. Even in the absence of bsp-RGD(15), BMSCs proliferated well within the softer gels (Figure 2A, top), while increases in peptide concentration enhanced cellular proliferation within the stiffer gels (Figure 2A, bottom). All variations of the 4% peptide crosslinked gel demonstrated substantial proliferation after 1 week (Figure 2A, middle). The end cell density data from these nine curves are reflected in the generated response surface that maps the cellular proliferation response as a function of both stiffness (taken from a frequency of 1Hz) and bsp-RGD(15) content (Figure 2B).

Fluorescence microscopy of these samples (Figure 2, C-H) shows sparse (due to low initial seeding density), but proliferating cells within the matrix with morphology dependent on the matrix composition. In the softest gels with no conjugated bsp-RGD(15), BMSCs grew in cell aggregates, without spreading, indicating that cell–cell interaction was favored over cell-matrix interaction. With the addition of bsp-RGD(15), cell association diminished, as did cell proliferation. These observations indicated that the addition of an integrin-engaging peptide influenced the interaction of cells with the matrix, but was not sufficient on its own to induce cell proliferation. As the matrix stiffness increased, cell spreading, as detected by light microscopy, was more abundant, and proliferation was stable across a range of peptide concentrations. However, at the highest stiffness, in which proliferation increased with increasing bsp-RGD(15) concentration, extensive cell spreading was visible within the high peptide concentration hydrogels. Thus, the matrix organizes cells in two distinct ways: when the modulus and ligand concentrations were low, cell-cell adhesion and proliferation as cell aggregates was dominant; when the modulus and ligand density were high, cell-matrix adhesion was preferred and proliferation occurred as single dispersed cells within the matrix.

Selection of the hydrogel for use in the mouse model was based on these results. Ideally, a 5 wt% formulation with high bsp-RGD(15) concentration would have been used. Limitations in the animal model, however, such as the thin wall of the murine heart and the subsequent need for a small gauge needle, influenced the choice of hydrogel. A 4 wt% formulation was chosen that had a lower modulus and that was more easily injected into the infarcted mouse heart. At this polymer content, 2 week proliferation was less dependent on bsp-RGD(15) concentration, so a midrange concentration (50 μM) was used (identified in Fig. 2B as a black circle).

Murine Infarct model

Matrix injection into the myocardium was well tolerated, with similar operational mortality compared to infarct generation and saline injection. In addition, no ventricular arrhythmias were observed with either cell or matrix injection. Matrix injection and cell transplantation had measurable effects on ventricular function, as reflected in echocardiographic assessment after acute MI (Table 2 and Figure 3). LV function in control infarcted hearts that were

injected with saline alone was significantly reduced in comparison to sham surgery animals, but did not change significantly over the time course studied. In contrast, while hearts receiving sIPN injection alone also had decreased function compared to sham initially, they experienced a gradual improvement in FS and EF, and at six weeks had functional levels that were numerically lower, but no longer statistically significantly different from sham-operated, uninfarcted animals. All groups with cell injection, either alone, with sIPNs, or with Matrigel™, displayed a numerical but not statistically significant improvement in FS, EF, and LVEDV compared to saline injection at 2 weeks. However, in these groups there was a progressive decline in LV function at later time points (Table 2 and Figure 3), and at six weeks, FS and EF were similar to saline controls. Comparing the differences in paired animal measurements (Figure 4) showed that all the groups with cells had a numerical decrease in function between 2 and 6 week time points.

Histological Examination

GFP-positive cells were detected in 38% of the hearts after injection with sIPN, while none were observed in the hearts undergoing injection of cells alone. Donor cells were detected in 25% of hearts after Matrigel™-enhanced transplantation. All GFP-positive cells at 6 weeks were localized to the area of injection near the infarct (Figure 5). An increase in wall thickness and preservation of myocardial cells in the infarct region was observed for hearts treated with sIPN alone compared to hearts injected with saline control (Figure 6).

Pooled Analysis of Cell Groups and Border Zone Placement

Significant differences were observed in comparisons of pooled data from treatment groups that received cells and those that did not (Figure 5). At two weeks, the addition of cells resulted in a significantly higher FS (45.6% versus 39.8%, $p < 0.05$) and a numerically higher EF (73.7% versus 67.5%, NS) than no cells, while at 6 weeks function was worse in hearts that received stem cells for both FS (34.2% versus 42.5%, $p < 0.05$) (Figure 7) and EF (62.7 versus 76.0, $p < 0.05$).

Given the technical limitations on the accuracy of injection site relative to eventual border zone formation in this murine model, we attempted to assess the impact of this variability in a subgroup analysis of specimens in which we found definitive histologic confirmation of border zone injection of matrix either alone or with cells (n=8, 4 Matrigel™, 4 sIPN). By aggregating all recipients of a confirmed border zone injection, thinning of the infarct region was found to be reduced compared to the animals without confirmation of border zone injections (n=24). In addition, FS and EF were found to be numerically, though not statistically, higher at 6 weeks in recipients of border zone injections compared to animals without observable material added to the border zone, and trends toward improvements in both infarct size and the thickness of the remote uninjured myocardium were also observed (Table 3).

Discussion

In this study, highly tunable synthetic injectable hydrogels were designed with a range of mechanical and biological properties that yielded different cellular responses *in vitro*. These *in vitro* data were then used to identify specific formulations that promoted the survival of transplanted cells and/or could provide mechanical stabilization to an injured ventricular wall. *In vivo* studies confirmed that these fully synthetic systems can be injected directly into the beating ventricle after ischemic injury without causing arrhythmias, and in comparison to non-degradable gels we have previously implanted in the myocardium they remodel with minimal foreign tissue responses and are no longer visible as bulk gel by 6 weeks (unpublished result). These matrices improved the survival of a population of transplanted

stem cells and could be useful for providing mechanical stabilization of the ventricle as a stand alone treatment.

While not statistically significant in our study, compared with other published studies using passive materials, we observed similar quantitative increases in ventricle function with the direct injection of the sIPNs. The lack of significance was due to the size and number of comparisons in our study, and the inherent variability in the *in vivo* metrics used, as a simple t-test comparing the saline to the sIPN at six weeks was significant on its own ($p<0.05$). Beneficial effects may initially be mechanical in nature, as even small amounts of added non contractile material in an infarct injured heart may be able to significantly reduce elevated fiber stress according to theoretical models we have developed.[22] As high border zone stresses have been implicated in chronic post-MI remodeling,[42,43] by reducing this myofiber mechanical dysfunction, the deterioration of the ventricle after a major ischemic event may be minimized or even reversed. The trends we and others[16,19,26-28] have observed with injections of the various hydrogels without any stem cells or growth factors provides early support for the published theoretical results, and the hypothesized impact of matrix injection on longer-term LV remodeling. The subgroup analysis of successful border zone injection further strengthens this hypothesis, and is in line with other studies which demonstrate that using biomaterials such as pNIPAAm based polymers, [26,28] Matrigel™,[13] collagen,[27] fibrin, [16] alginate[24,25] in the infarct injured heart improves mechanical behavior and potentially reduces pathological remodeling.

An alternate hypothesis for the noted improvements in ventricle function associated with synthetic materials was originally hypothesized by Fujiwara and co-workers who suggested that postinfarct inhibition of apoptosis might preserve myofibroblasts and endothelial cells in granulation tissue and modulate chronic left ventricular remodeling and heart failure.[44,45] Recent experiments using a biodegradable cardiac patch and injectable pNIPAAm hydrogels appear to demonstrate that enhancing the presence of granulation tissue during the inflammatory phase, and temporal extension of this phase, induced by the patch material, leads to improvement in cardiac function.[28,46] Furthermore, there may be an angiogenic effect and a tissue generating response from transient inflammation brought about by the host response to an implanted degradable material.[28] These effects could help to salvage the organ as any neotissue could provide mechanical support and increased blood perfusion to the at risk area could prevent the continued loss of functional tissue. Although the hypothesis is controversial, its validity cannot be discounted based on experimental evidence, and that it is impossible to avoid a mild inflammatory response to any material implanted in the heart. Further research, including more detailed modeling, *in vivo* testing with large animals, and histological tracking of implanted materials is obviously needed to better elucidate the mechanism of improvement.

Although a host of materials have shown promise in stabilization of the ventricle, most materials used have not been not ideal for cardiac tissue engineering applications. Some, such as Matrigel™, are derived biologically, and therefore pose potential problems of disease transmission, purity and reproducibility in large-scale manufacturing. Others have poorly controlled degradation profiles, or, like alginate, require calcium to gel, which may lead to local calcification by themselves or with the use of transplanted cells.[47] Most importantly, none of the materials, even the other NIPAAm based formulations,[26,28] used in these previous studies lend themselves to systematic optimization both mechanically and biologically, as precise modification of the various substrates is difficult. The material platform used in the present study provides potentially significant advancement in cardiac tissue engineering applications. The wide orthogonal control over both mechanical and biological properties of this injectable material allow for tuning the material for the specific application, presenting bioactive peptides for engagement and angiogenesis to the local

tissue, matching the degradation mode of the implant to the specific local MMP production, and choosing the material stiffness to provide an adequate growth structure for transplanted cells.

In contrast to the positive results with the use of a biomaterial alone in our animal model, the transplantation of BMSCs provided a transient improvement at 2 weeks but was associated with a negative trend over the course of the study. Although previous reports of stem cell transplantation using natural matrix products such as Matrigel™ have not described this transient benefit, our data are consistent with early time points from those reports. Kofidis *et al*,[13] followed hearts for only two weeks after Matrigel™-assisted cell transplantation. We also demonstrated a similar early benefit after cell injection, but found that this benefit was consistently lost at later time points. Furthermore, Kutshka *et al.*'[18] observed in a working heterotopic heart transplant model that *ex vivo* cell transplantation, alone or with either a Matrigel™ or collagen matrix, yielded a trend similar to that observed in this work. In that study, FS was increased at 2 weeks in all four groups undergoing cell transplantation. The average FS in each of these groups, however, decreased by week 4, at a time when the average FS had increased in the groups receiving matrix alone. More recently, Landa *et al*[19] also observed that FS at 8 weeks was not statistically significant from baseline for infarcts treated with neonatal cardiomyocytes, supporting the results in this work.

Although we cannot exclude the possibility that our results are specific to the type of cell used, the transient nature of the functional benefit we observed with cell transplantation is consistent with the published literature, and leads one to question why cell transplantation may not yield a sustained improvement in myocardial performance. One limitation to achieving long-term benefit is the failure to obtain true regeneration of functional tissue through survival, differentiation, and integration of donor cells in the host myocardium. Regression of early benefit may also be related to the rapid loss of the majority of transplanted cells, reported by many groups to occur within days after transplantation. This not only limits the cells available for integration, but also limits their anti-apoptotic effect via paracrine mechanisms.[48,49] Death of transplanted cells might even be directly detrimental to the myocardium through exacerbation of inflammatory signals or other biochemical sequelae.

The enhancement of longer-term survival of at least a fraction of cells that we observed with matrix-assisted transplantation provides an intriguing opportunity to overcome these limitations. Although the degree of enhanced survival observed with either natural or first-generation synthetic matrices was adequate to sustain early functional benefit, the tunable, easily engineered nature of synthetic matrices represent a critical advantage over naturally occurring matrices that cannot easily be modified or redesigned. While the complexity of the material presented may make short term clinical translation difficult compared to simpler systems, the orthogonal control of degradation, mechanical properties and biological functionality makes this a material an excellent choice for hypothesis driven testing in cardiac tissue engineering. While clinical delivery may be difficult, requiring cooled catheter based systems due to the stiffening upon warming to body temperature, as a test system, control of a wide latitude of parameters will allow for determining key functionality of cardiac tissue engineering materials, after which the material could be re-engineered into a simpler state containing the key functionality to allow for clinical application both in acute LV treatment and potentially for non-acute injuries such as the globally failing LV.

Acknowledgments

This work was supported in part by the American Heart Association (California Affiliate 20082098), and the National Institute of Health (1R01 HL083118-01 and 1K08 HL079239-01).

References

1. Orlic D, Kajstura J, Chimenti S, Limana F, Jakoniuk I, Quaini F, Nadal-Ginard B, Bodine DM, Leri A, Anversa P. Mobilized bone marrow cells repair the infarcted heart, improving function and survival. Proceedings of the National Academy of Sciences of the United States of America. 2001; 98(18):10344–10349. [PubMed: 11504914]
2. Hamano K, Li TS, Kobayashi T, Hirata K, Yano M, Kohno M, Matsuzaki M. Therapeutic angiogenesis induced by local autologous bone marrow cell implantation. Annals of Thoracic Surgery. 2002; 73(4):1210–1215. [PubMed: 11996265]
3. Tomita S, Mickle DAG, Weisel RD, Jia ZC, Tumiati LC, Allidina Y, Liu P, Li RK. Improved heart function with myogenesis and angiogenesis after autologous porcine bone marrow stromal cell transplantation. Journal Of Thoracic And Cardiovascular Surgery. 2002; 123(6):1132–1140. [PubMed: 12063460]
4. Kawamoto A, Tkebuchava T, Yamaguchi JI, Nishimura H, Yoon YS, Milliken C, Uchida S, Masuo O, Iwaguro H, Ma H, et al. Intramyocardial transplantation of autologous endothelial progenitor cells for therapeutic neovascularization of myocardial ischemia. Circulation. 2003; 107(3):461–468. [PubMed: 12551872]
5. Mangi AA, Noiseux N, Kong DL, He HM, Rezvani M, Ingwall JS, Dzau VJ. Mesenchymal stem cells modified with Akt prevent remodeling and restore performance of infarcted hearts. Nature Medicine. 2003; 9(9):1195–1201.
6. Wollert KC, Meyer GP, Lotz J, Ringes-Lichtenberg S, Lippolt P, Breidenbach C, Fichtner S, Korte T, Hornig B, Messinger D, et al. Intracoronary autologous bone-marrow cell transfer after myocardial infarction: the BOOST randomised controlled clinical trial. Lancet. 2004; 364(9429): 141–148. [PubMed: 15246726]
7. Meyer GP, Wollert KC, Lotz J, Steffens J, Lippolt P, Fichtner S, Hecker H, Schaefer A, Arseniev L, Hertenstein B, et al. Intracoronary bone marrow cell transfer after myocardial infarction - Eighteen months' follow-up data from the randomized, controlled BOOST (BOne marrOw transfer to enhance ST-elevation infarct regeneration) trial. Circulation. 2006; 113(10):1287–1294. [PubMed: 16520413]
8. Kang HJ, Kim HS, Zhang SY, Park KW, Cho HJ, Koo BK, Kim YJ, Lee DS, Sohn DW, Han KS, et al. Effects of intracoronary infusion of peripheral blood stem-cells mobilised with granulocyte-colony stimulating factor on left ventricular systolic function and restenosis after coronary stenting in myocardial infarction: the MAGIC cell randomised clinical trial. Lancet. 2004; 363(9411):751–756. [PubMed: 15016484]
9. Fuchs S, Baffour R, Zhou YF, Shou M, Pierre A, Tio FO, Weissman NJ, Leon MB, Epstein SE, Kornowski R. Transendocardial delivery of autologous bone marrow enhances collateral perfusion and regional function in pigs with chronic experimental myocardial ischemia. Journal Of The American College Of Cardiology. 2001; 37(6):1726–1732. [PubMed: 11345391]
10. Orlic D, Kajstura J, Chimenti S, Bodine DM, Leri A, Anversa P. Transplanted adult bone marrow cells repair myocardial infarcts in mice. Hematopoietic Stem Cells 2000 Basic And Clinical Sciences. 2001:221–230.
11. Beltrami AP, Barlucchi L, Torella D, Baker M, Limana F, Chimenti S, Kasahara H, Rota M, Musso E, Urbanek K, et al. Adult cardiac stem cells are multipotent and support myocardial regeneration. Cell. 2003; 114(6):763–776. [PubMed: 14505575]
12. Smith RR, Barile L, Cho HC, Leppo MK, Hare JM, Messina E, Giacomello A, Abraham MR, Marban E. Regenerative potential of cardiosphere-derived cells expanded from percutaneous endomyocardial biopsy specimens. Circulation. 2007; 115(7):896–908. [PubMed: 17283259]
13. Kofidis T, Lebl DR, Martinez EC, Hoyt G, Tanaka M, Robbins RC. Novel injectable bioartificial tissue facilitates targeted, less invasive, large-scale tissue restoration on the beating heart after myocardial injury. Circulation. 2005; 112(9):I173–I177. [PubMed: 16159811]
14. Toma C, Pittenger MF, Cahill KS, Byrne BJ, Kessler PD. Human Mesenchymal Stem Cells Differentiate to a Cardiomyocyte Phenotype in the Adult Murine Heart. Circulation. 2002; 105(1): 93–98. [PubMed: 11772882]
15. Laflamme MA, Chen KY, Naumova AV, Muskheli V, Fugate JA, Dupras SK, Reinecke H, Xu CH, Hassanipour M, Police S, et al. Cardiomyocytes derived from human embryonic stem cells in

pro-survival factors enhance function of infarcted rat hearts. Nature Biotechnology. 2007; 25(9): 1015–1024.

16. Christman KL, Fok HH, Sievers RE, Fang QH, Lee RJ. Fibrin glue alone and skeletal myoblasts in a fibrin scaffold preserve cardiac function after myocardial infarction. Tissue Engineering. 2004; 10(3-4):403–409. [PubMed: 15165457]
17. Kleinman HK, McGarvey ML, Liotta LA, Robey PG, Tryggvason K, Martin GR. Isolation and Characterization of Type-Iv Procollagen, Laminin, and Heparan-Sulfate Proteoglycan from the Ehs Sarcoma. Biochemistry. 1982; 21(24):6188–6193. [PubMed: 6217835]
18. Kutschka I, Chen IY, Kofidis T, Arai T, von Degenfeld G, Sheikh AY, Hendry SL, Pearl J, Hoyt G, Sista R, et al. Collagen matrices enhance survival of transplanted cardiomyoblasts and contribute to functional improvement of ischemic rat hearts. Circulation. 2006; 114:I167–I173. [PubMed: 16820568]
19. Landa N, Miller L, Feinberg MS, Holbova R, Shachar M, Freeman I, Cohen S, Leor J. Effect of injectable alginate implant on cardiac remodeling and function after recent and old infarcts in rat. Circulation. 2008; 117(11):1388–1396. [PubMed: 18316487]
20. Davis ME, Hsieh PCH, Grodzinsky AJ, Lee RT. Custom design of the cardiac microenvironment with biomaterials. Circulation Research. 2005; 97(1):8–15. [PubMed: 16002755]
21. Davis ME, Motion JPM, Narmoneva DA, Takahashi T, Hakuno D, Kamm RD, Zhang SG, Lee RT. Injectable self-assembling peptide nanofibers create intramyocardial microenvironments for endothelial cells. Circulation. 2005; 111(4):442–450. [PubMed: 15687132]
22. Wall ST, Walker JC, Healy KE, Ratcliffe MB, Guccione JM. Theoretical impact of the injection of material into the myocardium - A finite element model simulation. Circulation. 2006; 114(24): 2627–2635. [PubMed: 17130342]
23. Dai W, W LE, Dow JS, Kloner RA. Thickening of the infarcted wall by collagen injection improves left ventricular function in rats: a novel approach to preserve cardiac function after myocardial infarction. Journal Of The American College Of Cardiology. 2005; 46(4):714–719. [PubMed: 16098441]
24. Tsur-Gang O, Ruvinov E, Landa N, Holbova R, Feinberg MS, Leor J, Cohen S. The effects of peptide-based modification of alginate on left ventricular remodeling and function after myocardial infarction. Biomaterials. 2009; 30(2):189–195. [PubMed: 18849071]
25. Yu J, Gu Y, Du K, Mihardja S, Sievers RE, Lee RJ. The effect of injected RGD modified alginate on angiogenesis and left ventricular function in a chronic rat infarct model. Biomaterials. 2009; 30(5):751–756. [PubMed: 19010528]
26. Wang T, Wu DQ, Jiang XJ, Zhang XZ, Li XY, Zhang JF, Zheng ZB, Zhuo RX, Jiang H, Huang CX. Novel thermosensitive hydrogel injection inhibits post-infarct ventricle remodelling. European Journal of Heart Failure. 2009; 11(1):14–19. [PubMed: 19147452]
27. Jiang XJ, Wang T, Li XY, Wu DQ, Zheng ZB, Zhang JF, Chen JL, Peng B, Jiang H, Huang CX, et al. Injection of a novel synthetic hydrogel preserves left ventricle function after myocardial infarction. Journal of Biomedical Materials Research Part A. 2009; 90A(2):472–477. [PubMed: 18546187]
28. Fujimoto KL, Ma ZW, Nelson DM, Hashizume R, Guan JJ, Tobita K, Wagner WR. Synthesis, characterization and therapeutic efficacy of a biodegradable, thermoresponsive hydrogel designed for application in chronic infarcted myocardium. Biomaterials. 2009; 30(26):4357–4368. [PubMed: 19487021]
29. Stile RA, Healy KE. Thermo-responsive peptide-modified hydrogels for tissue regeneration. Biomacromolecules. 2001; 2(1):185–194. [PubMed: 11749171]
30. Kim S, Healy KE. Synthesis and characterization of injectable poly(N-isopropylacrylamide-co-acrylic acid) hydrogels with proteolytically degradable cross-links. Biomacromolecules. 2003; 4(5):1214–1223. [PubMed: 12959586]
31. Kim S, Chung EH, Gilbert M, Healy KE. Synthetic MMP-13 degradable ECMs based on poly(N-isopropylacrylamide-co-acrylic acid) semi-interpenetrating polymer networks. I. Degradation and cell migration. Journal of Biomedical Materials Research Part A. 2005; 75A(1):73–88. [PubMed: 16049978]

32. Chung EH, Gilbert M, Virdi AS, Sena K, Sumner DR, Healy KE. Biomimetic artificial ECMs stimulate bone regeneration. Journal of Biomedical Materials Research Part A. 2006; 79A(4):815–826. [PubMed: 16886222]
33. Bellahcene A, Bonjean K, Fohr B, Fedarko NS, Robey FA, Young MF, Fisher LW, Castronovo V. Bone sialoprotein mediates human endothelial cell attachment and migration and promotes angiogenesis. Circulation Research. 2000; 86(8):885–891. [PubMed: 10785511]
34. Engler A, Bacakova L, Newman C, Hategan A, Griffin M, Discher D. Substrate compliance versus ligand density in cell on gel responses. Biophysical Journal. 2004; 86(1):617–628. [PubMed: 14695306]
35. Engler AJ, Sen S, Sweeney HL, Discher DE. Matrix elasticity directs stem cell lineage specification. Cell. 2006; 126(4):677–689. [PubMed: 16923388]
36. Saha K, Keung AJ, Irwin EF, Li Y, Little L, Schaffer DV, Healy KE. Substrate Modulus Directs Neural Stem Cell Behavior. Biophysical Journal. 2008; 95(9):4426–4438. [PubMed: 18658232]
37. Kamide, K. Phase equilibria and critical phenomena. Elseveir Science Publishers; Amsterdam: 1990. Thermodynamics of polymer solutions.
38. Stile RA, Burghardt WR, Healy KE. Synthesis and characterization of injectable poly(N-isopropylacrylamide)-based hydrogels that support tissue formation in vitro. Macromolecules. 1999; 32(22):7370–7379.
39. Peterson JT, Li H, Dillon L, Bryant JW. Evolution of matrix metalloprotease and tissue inhibitor expression during heart failure progression in the infarcted rat. Cardiovascular Research. 2000; 46(2):307–315. [PubMed: 10773235]
40. Deng SJ, Bickett DM, Mitchell JL, Lambert MH, Blackburn RK, Carter HL, Neugebauer J, Pahel G, Weiner MP, Moss ML. Substrate specificity of human collagenase 3 assessed using a phage-displayed peptide library. Journal of Biological Chemistry. 2000; 275(40):31422–31427. [PubMed: 10906330]
41. Huebsch N, Gilbert M, Healy KE. Analysis of sterilization protocols for peptide-modified hydrogels. Journal of Biomedical Materials Research Part B-Applied Biomaterials. 2005; 74B(1): 440–447.
42. Grossman W, Jones D, McLaurin LP. Wall Stress And Patterns Of Hypertrophy In Human Left-Ventricle. Journal Of Clinical Investigation. 1975; 56(1):56–64. [PubMed: 124746]
43. Jackson BM, Gorman JH, Moainie SL, Guy TS, Narula N, Narula J, John-Sutton MG, Edmunds LH, Gorman RC. Extension of borderzone myocardium in postinfarction dilated cardiomyopathy. Journal Of The American College Of Cardiology. 2002; 40(6):1160–1167. [PubMed: 12354444]
44. Takernura G, Fujiwara H. Morphological aspects of apoptosis in heart diseases. Journal of Cellular and Molecular Medicine. 2006; 10(1):56–75. [PubMed: 16563222]
45. Hayakawa K, Takemura G, Kanoh M, Li YW, Koda M, Kawase Y, Maruyama R, Okada H, Minatoguchi S, Fujiwara T, et al. Inhibition of granulation tissue cell apoptosis during the subacute stage of myocardial infarction improves cardiac remodeling and dysfunction at the chronic stage. Circulation. 2003; 108(1):104–109. [PubMed: 12821555]
46. Fujimoto KL, Tobita K, Merryman WD, Guan JJ, Momoi N, Stolz DB, Sacks MS, Keller BB, Wagner WR. An elastic, biodegradable cardiac patch induces contractile smooth muscle and improves cardiac remodeling and function in subacute myocardial infarction. Journal of the American College of Cardiology. 2007; 49(23):2292–2300. [PubMed: 17560295]
47. Breitbach M, Bostani T, Roell W, Xia Y, Dewald O, Nygren JM, Fries JWU, Tiemann K, Bohlen H, Hescheler J, et al. Potential risks of bone marrow cell transplantation into infarcted hearts. Blood. 2007; 110(4):1362–1369. [PubMed: 17483296]
48. Mirotsou M, Zhang ZY, Deb A, Zhang LN, Gnecchi M, Noiseux N, Mu H, Pachori A, Dzau V. Secreted frizzled related protein 2 (Sfrp2) is the key Akt-mesenchymal stem cell-released paracrine factor mediating myocardial survival and repair. Proceedings of the National Academy of Sciences of the United States of America. 2007; 104(5):1643–1648. [PubMed: 17251350]
49. Xu MF, Uemura R, Dai Y, Wang YG, Pasha Z, Ashraf M. In vitro and in vivo effects of bone marrow stem cells on cardiac structure and function. Journal of Molecular and Cellular Cardiology. 2007; 42(2):441–448. [PubMed: 17187821]

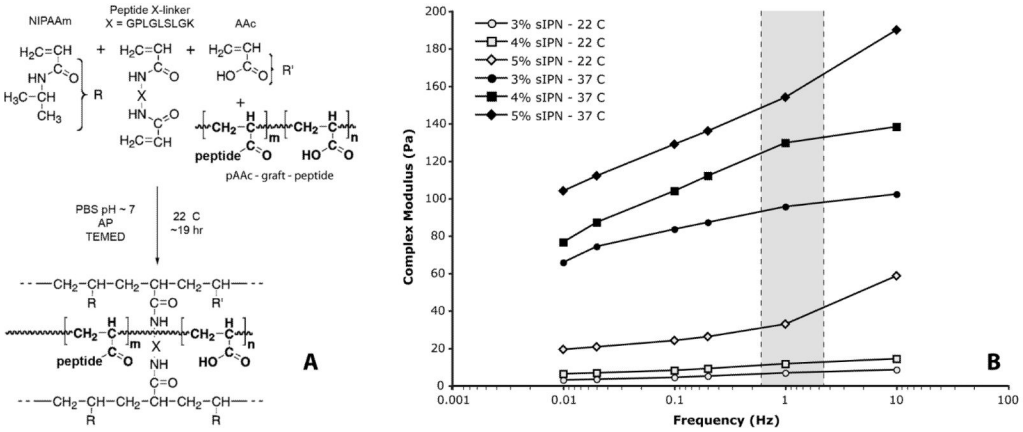

Figure 1.

Polymer synthesis scheme for sIPN thermoresponsive, MMP degradable, peptide modified synthetic ECM hydrogel (**A**). Complex modulus as a function of temperature, frequency, and composition of the sIPN hydrogels (**B**). Gray zone indicates cardiac tissue engineering range of frequency loadings.

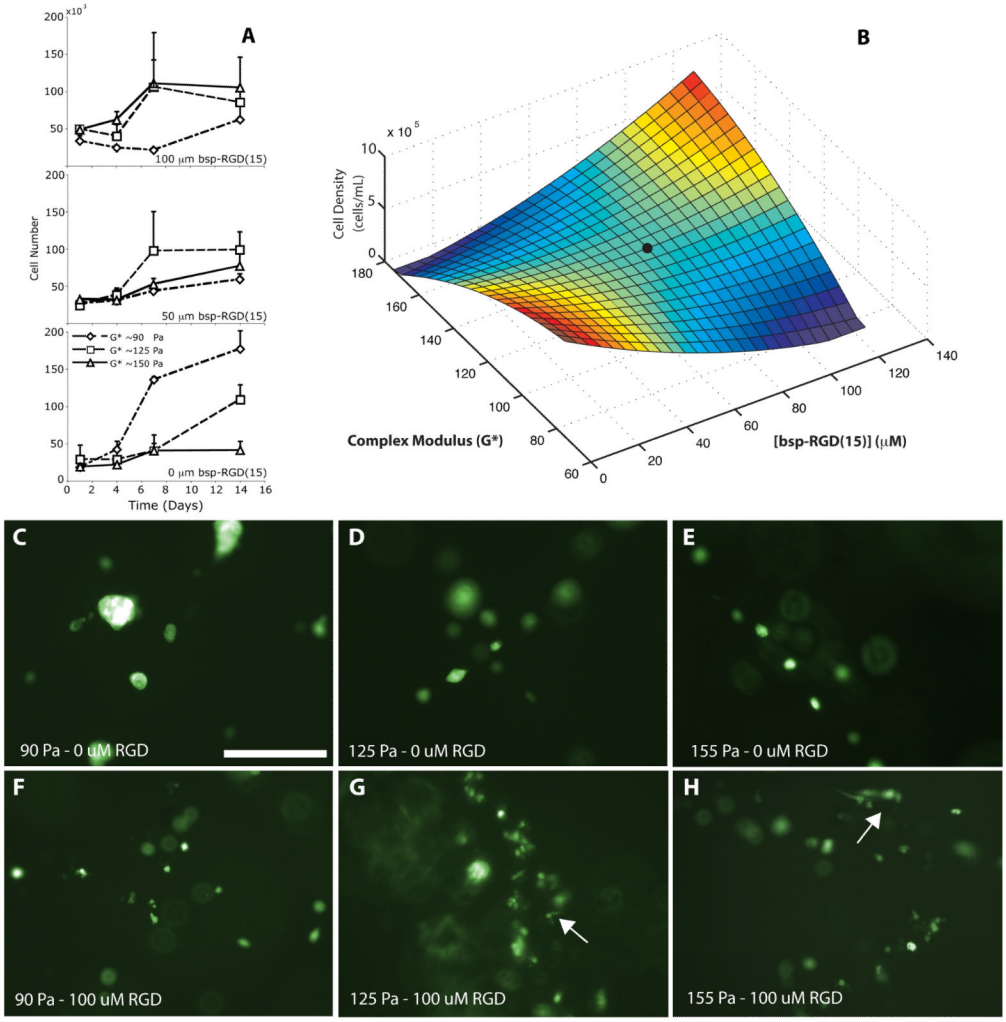

Figure 2.

Time course of cellular growth in the sIPN matrix as a function of bsp-RGD(15) concentration and matrix stiffness (**A**). The cell vs. time data can be transformed into a response surface (t=14 days) by fitting the nine data points to a quadratic 3D surface, R^2=0.87 (**B**). The black circle indicates material composition used in the murine infarct model. Fluorescent microscopy of GFP-expressing BMSCs cultures *within* sIPNs after 14 days (**C-H**, scale bar = 250 μm). Low modulus-low bsp-RGD(15) conditions show growing clusters of multiple cells, while cell spreading can be seen in the high modulus, high bsp-RGD(15) conditions. Arrows indicate spreading cells within the gel.

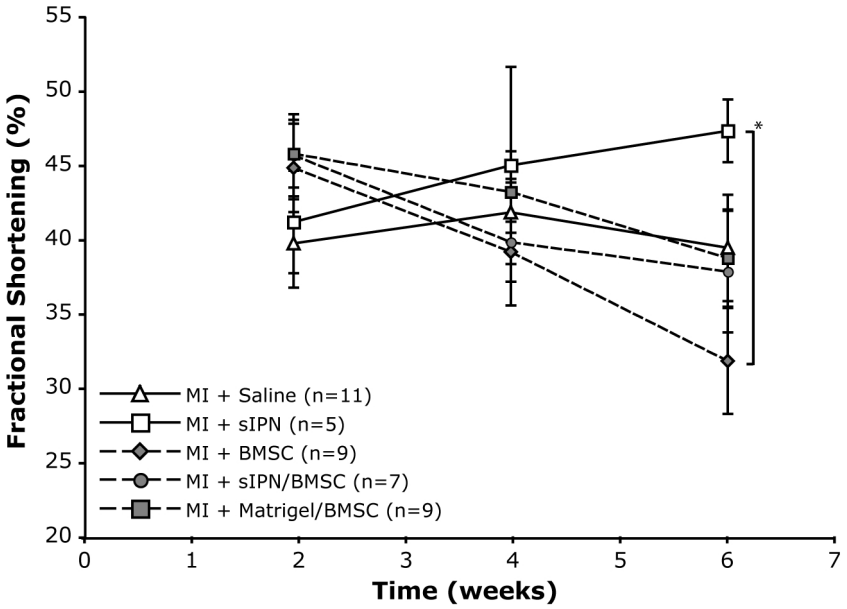

Figure 3.

FS data as a function of time for all animal groups. Solid lines indicate conditions without added cells while dashed lines represent groups with added cells. Error bars indicate SEM. Groups marked with a * have a $P < 0.05$ while all other groups are not statistically different. All data collected on non-anesthetized conscious gently restrained mice.

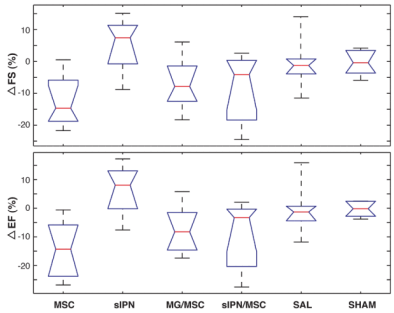

Figure 4.
Paired differences in animal data in FS and EF from 2 to 6 weeks. All groups with cells added show degradation of ventricular performance while sIPN treated ventricles increase in metrics.

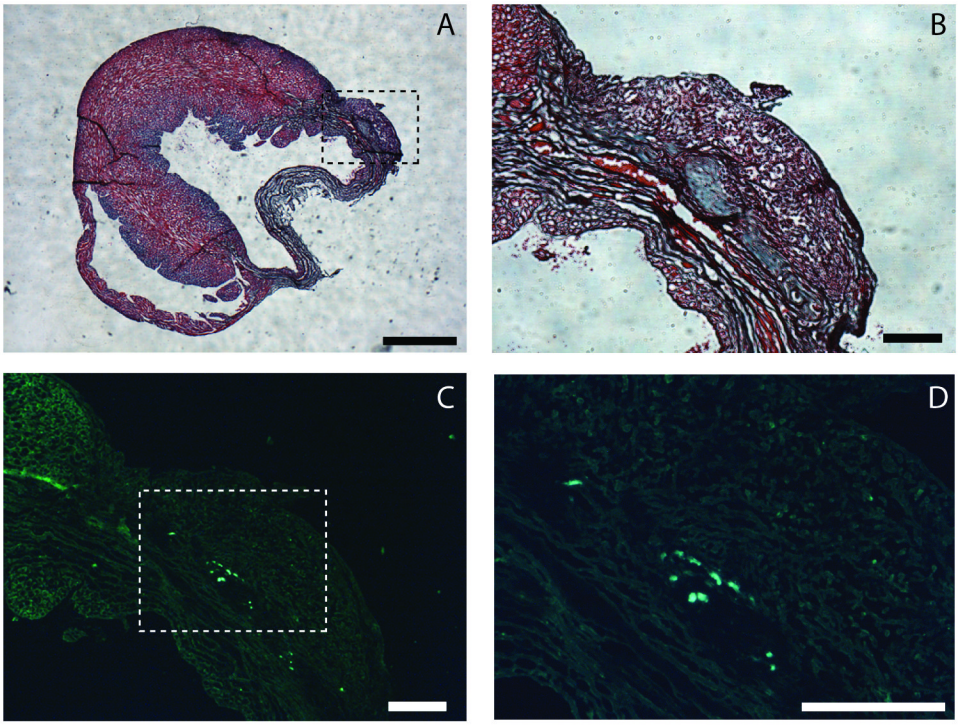

Figure 5.

Localization of injected sIPN and present GFP cells at t = 6 weeks. Gomori's Trichrome stained ventricle indicating region of injection (dashed box) and adjacent infarct,(**A**, scale bar = 1mm). Higher magnification (4×) of injection region reveals partially degraded and remodeled hydrogel (**B**, scale bar = 250 μm). Fluorescent image of the injection region (4×) indicates the presence of GFP-positive cells (**C**) in the injection site, and a higher magnification (10×) image of box of interest in C (dashed box) showing individual GFP positive cells (**D**, scale bar = 250 μm).

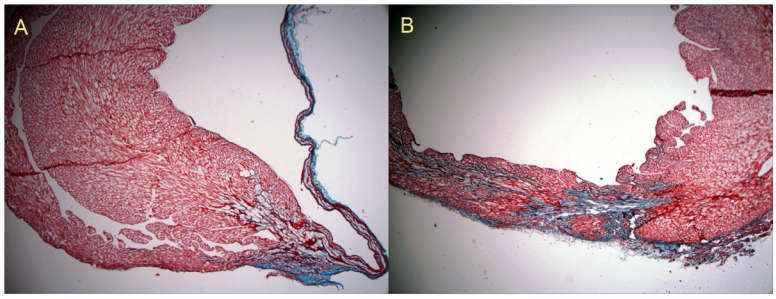

Figure 6.
Histological sections stained with Gomori's trichrome. Saline injections at 2.5× (**A**) demonstrate extensive thinning of the LV wall 6 weeks after the infarct. Treatment with an MMP-degradable sIPN in the infarct BZ demonstrates increased thickness of the LV wall and extensive remodeling of the LV wall at the site of injection (**B**, 2.5×).

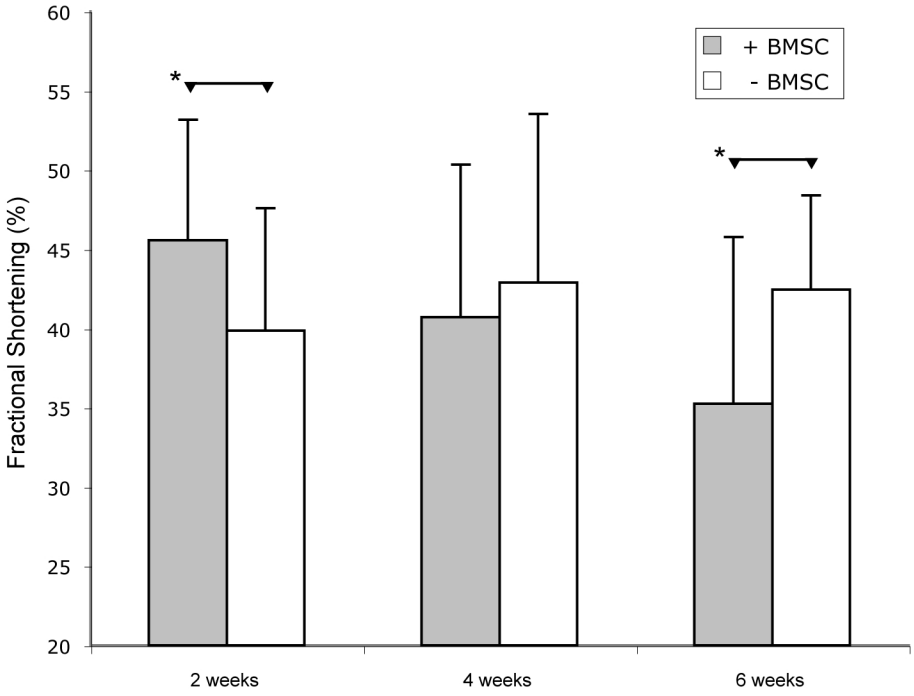

Figure 7.
Temporal changes in FS after a generated MI. Gray bars indicate mean of animals with BMSCs while white bars are animals without BMSCs. Error bars indicate standard deviation. Two week and six week pooled samples are statistically significant ($p<0.05$)

Table 1

Calculated Michaelis-Menten parameters for the tested crosslinking sequences (top) and selectivity ratios compared against the slowest degrading sequence (bottom).

		QPQGLAK (slow)		**GPLGLSLGK (med)**		**GPLGMHGK (fast)**	
	k_{cat} =	0.82	s^{-1}	14.1	s^{-1}	73.9	s^{-1}
MMP - 13	K_m =	1.1	*M*	317	*M*	465	*M*
	k_{cat}/K_m =	7.3 e2	$s^{-1}M^{-1}$	4.5 e4	$s^{-1}M^{-1}$	1.5 e5	$s^{-1}M^{-1}$
	k_{cat} =	25.4	s^{-1}	46.7	s^{-1}	167.8	s^{-1}
MMP - 9	K_m =	1223	*M*	940	*M*	727	*M*
	k_{cat}/K_m =	2.1 e4	$s^{-1}M^{-1}$	5.0 e4	$s^{-1}M^{-1}$	2.3 e5	$s^{-1}M^{-1}$
	k_{cat} =	36.5	s^{-1}	21.1	s^{-1}	620	s^{-1}
MMP-2	K_m =	2028	*M*	216	*M*	3558	*M*
	k_{cat}/K_m =	1.8 e4	$s^{-1}M^{-1}$	9.8e4	$s^{-1}M^{-1}$	1.7 e5	$s^{-1}M^{-1}$
MMP - 13	selectivity ratio	1		62		205	
MMP - 9	selectivity ratio	1		2.4		11	
MMP - 2	selectivity ratio	1		5.5		9.4	

Table 2

Echocardiography results for the various treatment groups collected on non-anesthetized conscious mice. Within the same time-point, all measurements were evaluated using a Tukey HSD multiple group comparison, and groups noted that are significantly different from the sham group (* P<0.05). Within the same treatment group, comparisons between time point were also evaluated (†P<0.05).

Measurements of Serial Echocardiography

	2-week			6-week		
	EF(%)	**FS(%)**	**LVEDV**	**EF(%)**	**FS(%)**	**LVEDV**
MSC	73.0±2.5*†	44.7±2.5*†	39.8±7.9	57.8±3.5*†	31.6±3.1*†	78.5±11.1
sIPN	68.1±3.4*	41.1±3.3*	60.1±10.6	75.4±4.9	47.3±4.4*	52.2±15.7
sIPN+MSC	74.0±2.5*	45.6±2.5*	45.7±7.9	66.2±4.0*	38.6±3.6*	68.3±12.8
me+MSC	74.0±3.8*	45.7±2.8*	46.7±8.9	65.2±3.7*	37.7±3.3*	72.9±11.9
Saline	68.1±3.1*	39.6±3.0*	56.6±9.6	67.9±4.0*	39.3±3.6*	55.1±12.8
Sham	85.9±3.0	59.8±3.0	30.5±8.8	85.6±3.7	59.5±3.3	30.3±11.9

J Biomed Mater Res A. Author manuscript; available in PMC 2011 December 15.

Table 3

Comparison between the animal subgroup which had clearly visible material (sIPN or Matrigel™) contained within the infarct border zone and the other animals. Only the infarct thickness was statistically significantly different ($p<0.05$) between groups with observable material in the border zone and those without.

Histological Measurements of Border Zone Placement

	+ BZ Material	- BZ Material
Infarct Thickness (mm)	0.40 ± 0.12	0.23 ± 0.15
Remote Thickness (mm)	1.14 ± 0.12	1.11 ± 0.21
Apical Infarct Area (%)	21.0 ± 12.0	31.0 ± 22.0
6 week FS (%)	41.0 ± 9.0	37.1 ± 11.4
6 week EF (%)	68.1 ± 9.7	65.4 ± 13.2
6 week LVEDV (%)	63.2 ± 20.8	69.7 ± 37.4